Hybrid Compounds

Supramolecular Coordination Assemblies of Dinuclear Fe^{III} Complexes**

Wolfgang Schmitt, Jonathan P. Hill, M. Paula Juanico, Andrea Caneschi, Ferdinando Costantino, Christopher E. Anson, and Annie K. Powell**

Dedicated to Professor Rüdiger Kniep on the occasion of his 60th birthday

Construction of 3D architectures as well as molecular recognition processes are regarded as key aspects of modern supramolecular chemistry.[1] The ability to produce hierarchically ordered structures by the self-assembly of oligomeric subunits is of importance for potential applications.[2] This self-assembly requires a detailed knowledge of the competing structure-directing forces present within the reaction systems. Furthermore, it requires the ability to tune these interactions by consideration of steric restrictions and the nature and specific affinities of the chemical components.

Hybrid organic–inorganic coordination assemblies represent a distinct class of supramolecular compound whose preparation is currently a very active area in chemical and materials research.[3] Hybrid organic–inorganic materials present a means for customizing physical and chemical properties by reducing dimensionality and by influencing the devolution pattern of classical inorganic materials within their crystal structures. One strategy for the synthesis of such

[*] Dr. W. Schmitt, Dr. J. P. Hill, Dr. M. P. Juanico, Dr. C. E. Anson, Prof. Dr. A. K. Powell
Institut für Anorganische Chemie
Universität Karlsruhe
Engesserstrasse Geb. 30.45, 76128 Karlsruhe (Germany)
Fax: (+49) 721-608-8142
E-mail: schmitt.wolfgang@nims.go.jp
powell@chemie.uni-karlsruhe.de

Dr. W. Schmitt, Dr. J. P. Hill
National Institute for Materials Science
ICYS Department
Tsukuba, 1-1 Namiki, Ibaraki 305 0044 (Japan)
Fax: (+81) 29-860-4708

Prof. Dr. A. Caneschi, F. Costantino
Dipartimento di Chimica and
UdR INSTM di Firenze
Polo Scientifico
Via della Lastruccia 3, 50019 Sesto Fiorentino (Fi) (Italy)

[**] This work was supported by the DFG "Center for Functional Nanostructures (CFN)", the Special Coordination Funds for Promoting Science and Technology from MEXT, Japan through ICYS Fellowships (W.S. and J.P.H.) and the EU-FP6 RTN QUEMOLNA and NOE MAGMANET (A.K.P., M.P.J., A.C., F.C.). Structural studies have been performed under the approval of the Photon Factory Program Advisory Committee (Proposal 04G238). We are grateful to T. Sasaki for assistance with TEM measurements.

Supporting information for this article (magnetic data for **5**, representative TGA data, additional presentations of the crystal structures) is available on the WWW under http://www.angewandte.org or from the author.

 DOI: 10.1002/ange.200500516

structures makes use of rigid organic complexing agents. By using metal atoms, oligonuclear complexes or clusters, and organic components with distinct morphologies as building blocks it is hoped to control the self-assembly process.[4] Using this approach it is not only possible to reconstruct classical inorganic structures but also to overcome the geometrical limitations of the classical aluminosilicates resulting in materials with unprecedented porosity. Construction of multidimensional M-O-M frameworks has been demonstrated to produce materials supporting cooperative effects in their inorganic regions and can also lead to improved thermal stability.[5] Careful selection of metal ions and ligands and consideration of their preferred coordination modes and geometries allows the construction of crystalline architectures containing 1D, 2D, and 3D M-O-M frameworks and a systematic investigation of their chemophysical properties.[5,6]

Herein we describe a concept for synthesis of hybrid organic–inorganic compounds where the shape and functionality of aromatic ligands determine the dimensions and architecture of the inorganic regions of the resulting hybrid materials. Our work emphasizes the structure-directing effects of iminodiacetic acid substituted phenols and similar naphthol derivatives (Scheme 1). These multidentate complexing agents contain hydrophilic and hydrophobic moieties

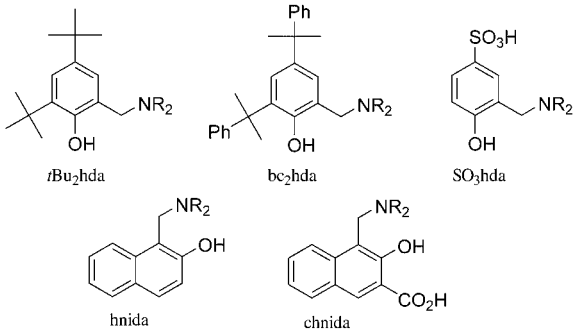

Scheme 1. The protonated organic ligands obtained by Mannich reaction on the appropriate phenol or naphthol; R = CH_2COOH.

and react with Fe^{III} salts to give dinuclear complexes where the transition-metal ions are doubly bridged by combinations of hydroxo-, oxo-, and carbonate groups. The resulting complexes, which form through hydrolysis reactions in the presence of specific amounts of water, can be described by the general formulae $[Fe_2(\mu\text{-}OH)(\mu\text{-}CO_3)L_2]^{3-}$, $[Fe_2(\mu\text{-}O)(\mu\text{-}CO_3)L_2]^{4-/6-}$, or $[Fe_2(\mu\text{-}CO_3)_2L_2]^{4-}$. The fixation of atmospheric CO_2 by transition-metal ions is now well-established.[7] Alkali counterions are bound to the negatively charged Fe^{III} complexes through the carboxylate groups and other O-donors. They are further linked to each other by water molecules forming supramolecular coordination assemblies. The hydrophilic/hydrophobic character of the reaction systems favors the formation of cross-linked structures in which self-assembling processes organize vast areas of different polarities.

The hydrolysis reactions in the presence of the tetradentate ligand tBu$_2$hda led to the crystallization of **1**.

$K_3[Fe_2(\mu\text{-}OH)(\mu\text{-}CO_3)(t\text{Bu}_2\text{hda})_2] \cdot 3\,H_2O \cdot EtOH$ **1**

The long Fe–O bond lengths of 2.002(3) and 2.007(4) Å to the bridging oxygen atom confirm the identity of this bridging ligand as a hydroxo group; the hydrogen atom could be located and refined in the crystal structure. This compound forms a two dimensional lamellar structure with potassium ions in the *ab* plane connected to the dinuclear Fe^{III} complexes above and below this plane while the organic residues of the Fe^{III} complexes point in the direction of the crystallographic *c* axis. In this direction the 2D layers bind to each other through weak induced dipole interactions forming organic regions approximately 11.5 Å thick. Similarly in **2**, the ligand hnida stabilizes a layered structure with organic and inorganic layers parallel to the crystallographic *bc* plane.

$K_4[Fe_2(\mu\text{-}O)(\mu\text{-}CO_3)(\text{hnida})_2] \cdot 6\,H_2O \cdot 2\,EtOH$ **2**

The Fe^{III} centers of the dinuclear complex in **2** are doubly bridged by a carbonate anion and an oxo ligand, which has significantly shorter bonds (both 1.81 Å) to the Fe^{III} centers than the corresponding hydroxo group in **1**. This oxygen also coordinates to two K^+ ions resulting in a distorted tetrahedral $Fe_2(\mu_4\text{-}O)K_2$ geometry. Figure 1 shows the dinuclear Fe^{III} subunits in **1** and **2** and the layered arrangements of hydrophobic and hydrophilic moieties. It is noteworthy that in **2** the dinuclear subunit straddles the hydrophilic layer while in **1** both organic ligand moieties of a given $[Fe_2(\mu\text{-}OH)(\mu\text{-}CO_3)(t\text{Bu}_2\text{hda})_2]^{3-}$ unit are accommodated in the same hydrophobic layer.

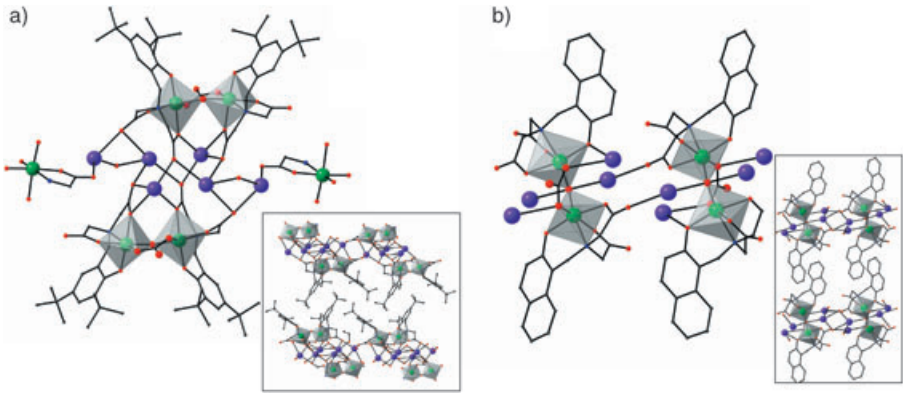

Figure 1. a) Layered arrangement of dinuclear Fe^{III} complexes in **1**. Inset: section of the structure of **1** viewed along the crystallographic *a*-axis. b) Structure of **2** illustrating the straddling of the hydrophilic layer by the dinuclear subunit. Inset: section of the structure of **2** viewed along the crystallographic *a*-axis. Hydrogen atoms and solvent molecules are omitted for clarity; Fe green, O red, N blue, K purple, C dark gray; coordination polyhedra of the Fe centers are shown in gray.

Modification of the tBu$_2$hda ligand by substitution of the *tert*-butyl groups with α,α-dimethylbenzyl groups increases the hydrophobicity of the complexing agent. The compound **3** crystallizes from aqueous systems containing the bc$_2$hda ligand, and dipole–dipole and dipole–cation interactions favor a layered structure similar to **1**. However, **3** has the additional feature of a π-bound potassium ion which is trapped within the hydrophobic part made up of the α,α-dimethylbenzyl groups (Figure 2).[8] This motif is attracting

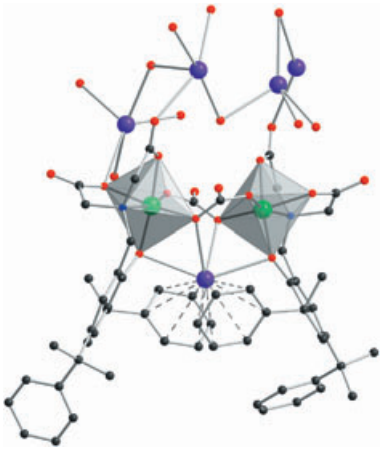

Figure 2. Coordination geometry of the Fe^{III} centers and the cation–π binding of potassium ions in complex **3**. Color code: Fe green, O red, N blue, K purple, C dark gray. Hydrogen atoms and solvent molecules are omitted for clarity.

interest because of its importance in protein dynamics although the near absence of structural evidence has made it difficult to visualize cation–π interactions involving alkali metal cations.[9]

$K_3[Fe_2(\mu\text{-}CO_3)_2(bc_2hda)_2] \cdot 3\,H_2O \cdot EtOH$ **3**

The π-binding of the potassium cation in **3** prompted us to consider further alterations to the ligand. Thus, we chose to introduce carboxylate or sulfonate groups, either of which can be placed at various positions on the ligand. We considered that these functional groups would influence the inorganic structural motif of the coordination assemblies and could create 2D or 3D networks. Introduction of a carboxy group at the 3-position of the naphthyl ring of (2-hydroxynaphthyl)-methylene iminodiacetic acid (hnida) gives the chnida ligand, which stabilizes another novel structural motif. In the resulting compound **4**, the dinuclear Fe^{III} complexes are arranged so that the polar oxo, carbonate, and carboxylate groups together with the water-bridged K$^+$ ions build a honeycomb structure containing channels running parallel to the crystallographic *c*-axis. Each dinuclear unit penetrates a honeycomb wall with the Fe···Fe axis approximately perpendicular to the *c* axis, whereas the naphthalene moieties of the two ligands project into adjacent channels of the lattice, where the naphthalene mean planes make angles of 40.7 and 51.4° to the *c* axis.

$K_6[Fe_2(\mu\text{-}O)(\mu\text{-}CO_3)(chnida)_2] \cdot 13.5\,H_2O$ **4**

The resulting hydrophobic channels are approximately 14 Å in diameter. In the chnida ligand, the carboxy group is positioned adjacent to the phenolic OH group maximizing the amphiphilicity of the ligand. As before, this enables complexes with this ligand to pack into a structure where hydrophobic and hydrophilic regions are segregated. However, in the structure of **4** it is almost as though the bilayer arrangement seen for **1**–**3** has been rolled up, leading to channels which contain the naphthyl residues (Figure 3 a).

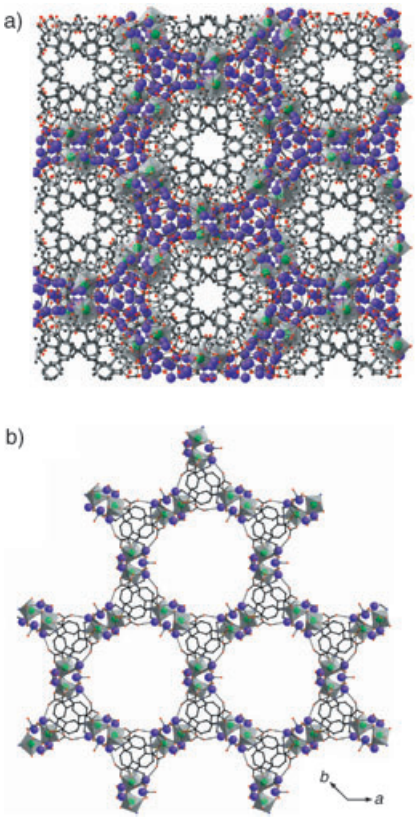

Figure 3. a) Honeycomb structural motif in **4**. Inorganic and organic parts form parallel nanosized channels which run along the crystallographic *c*-axis and which are filled with naphthyl moieties (view in [001] direction). b) Open framework structure in **5** viewed along the crystallographic *c*-axis. Hydrogen atoms, solvent molecules, and one disordered K$^+$ counterion are omitted for clarity; Fe green, O red, N blue, K purple, C dark gray.

This structure is the direct consequence of the introduction of the carboxy group adjacent to the phenolic OH group. This carboxy group does not coordinate to Fe^{III} ions but interacts only with the potassium counterions.

In addition to the single-crystal X-ray structure analysis, we performed high resolution transmission electron microscopy (HRTEM) on powdered samples of **4** to characterize the extended structure of the compound further. Although crystals of **4** are very sensitive to electron-beam-induced damage it was possible to observe areas displaying the expected honeycomb pattern, in good agreement with the crystal structure determination (Figure 4).

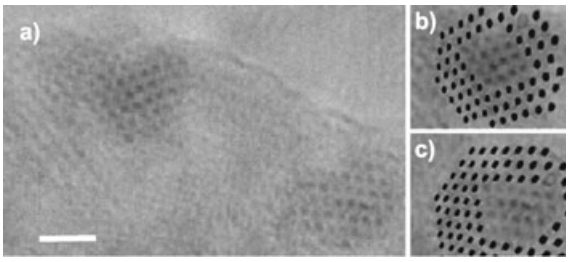

Figure 4. a) TEM image of **4** distinguishing the organic (dark) and inorganic (light) areas (scale bar 10 nm). b), c) Overlay of organic regions of the (110) plane of crystal structure on TEM image. Dot array was generated from the *hkl* file and adjusted for perspective.

To encourage the formation of materials containing pores or empty channels where the organic ligand is incorporated into an extended framework structure, we introduced a sulfonic acid group in the position *para* to the phenolic hydroxy group of the hda ligand so that the dinuclear unit could pillar between hydrophilic regions of supramolecular structures. This strategy yielded **5** in which five of the potassium cations are strongly bound by the oxo, carbonate, and carboxylate groups around the Fe_2 unit. Each ligand sulfonate group binds to the K^+ counterions of a neighboring dinuclear complex. In the resulting coordination assembly, the dinuclear complexes and K^+ ions form the walls of an open framework honeycomb motif, where the Fe_2 units are aligned within, rather than through the walls, as was found for **4**.

$K_6[Fe_2(\mu\text{-}O)(\mu\text{-}CO_3)(SO_3hda)_2]\cdot 11\,H_2O\cdot 9\,MeOH$ **5**

The aromatic rings of the dinuclear subunits are stacked about the threefold screw (3_2) axes which coincide with the vertices of this hexagonal structure (Figure 3b). The open framework structure has channels with cross-sectional diameter of approximately 9 Å, which contain water, methanol, and the disordered sixth potassium ion. Recently, other hybrid coordination assemblies have attracted interest as new catalytic materials[5e,10] or separation media.[2d,11] Compound **5** is a good example of the application of our concept in the synthesis of closely related compounds and it seems reasonable to expect the tailoring of channel geometry by variation of the dimensions and functionality of the ligand.

Magnetic susceptibility studies show that the dinuclear Fe^{III} units in these compounds are, as expected, fairly strongly antiferromagnetically coupled, presumably with the coupling transmitted through the μ-oxo bridge.[12] As an example, for compound **5** the room temperature χT value is 1.25 $cm^3\,K\,mol^{-1}$ per dinuclear unit (for two uncoupled Fe^{III} ions the value is $\chi T_{theor} = 8.75\ cm^3\,K\,mol^{-1}$) and decreases steeply on lowering the temperature. It then remains constant, but not zero, between 35 and 5 K as a result of the presence of a small amount of paramagnetic impurity (confirmed by magnetization experiments). The data can be reproduced quantitatively using a van Vleck law for a dimer of coupled $S = 5/2$ ions with the best fit for $J = -173 \pm 2\ cm^{-1}$ and allowing for the presence of less than 3% paramagnetic impurity (for full details see the Supporting Information).

The thermogravimetric analyses (TGA) reveal that the coordination assemblies decompose by initial solvent loss (below 150 °C) followed by degradation of the organic ligand at temperatures between 250 and 350 °C. The loss of the structural integrity is accompanied by the formation of potassium oxide and iron oxides. Weight losses at higher temperatures can be attributed to the solid-state reactions of this mixture forming different phases of potassium iron oxides. A detailed account of thermolysis and pyrolysis of the complexes and the structure of the decomposition products will be reported elsewhere. However, it is noteworthy that in the case of **1** we were able to identify $KFeO_2$ and the K-β-ferrite $K_xFe_{22}O_{34}$ ($x = 2$–4)[13] as the main products using X-ray diffraction (XRD) analysis of samples thermolyzed at different, increasing temperatures. $KFeO_2$ and $K_xFe_{22}O_{34}$ ($x = 2$–4) are the only thermodynamically stable ternary compounds in the K_2O-Fe_2O_3 system and usually form by reaction of Fe_2O_3 or Fe_3O_4 with K_2CO_3 or K_2O.[14] Recent work has suggested that the active state of the industrially used Fe_2O_3 dehydrogenation catalyst for the production of styrene from ethylbenzene consists of the $KFeO_2$ and $K_xFe_{22}O_{34}$ ($x = 2$–4) oxides.[15] Since the production of styrene is one of the most important industrial processes and reaches a production level of 20×10^6 tons/year,[16] nanostructured materials containing these oxides are of industrial interest.

In summary, our studies demonstrate that hydroxybenzyl iminodiacetic acid ligands can be used to prepare an unprecedented type of hybrid organic–inorganic network by self-assembly of the dinuclear doubly bridged Fe^{III} subunits and their potassium counterions, resulting in a variety of 3D architectures which are summarized in Scheme 2. The structure of the inorganic hydrophilic zone is strongly influenced by the shape and functionality of the organic ligand providing a means of controlling different motifs of supramolecular coordination assemblies. Selection of the ligand structure and polarity can result in crystalline materials where the packing of hydrophilic and hydrophobic portions differs from a simple bilayer arrangement. This approach has allowed formation of a dense hexagonal array (using the chnida ligand) and a

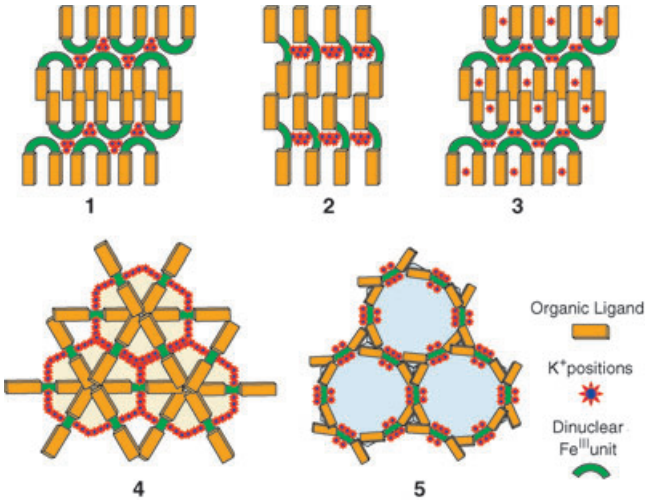

Scheme 2. Pictograms of structural motifs in the supramolecular coordination networks.

hexagonal open-framework structure containing cylindrical voids (using the SO_3hda ligand). Thermal decomposition of these and similar aggregates, which contain distinct areas of polarity and structure, can lead to unusual oxides whose structures and compositions depend on those of the precursor compound. In particular, we are seeking to prepare nanostructured mixed transition metal oxides whose properties may depart from those prepared by other techniques.

Experimental Section

All ligands were prepared by Mannich reaction between the appropriate phenol or naphthol, iminodiacetic acid and aqueous formaldehyde.[17]

1: Complex **1** was prepared by the reaction of Na_2tBu_2hda (0.198 g, 0.5 mmol) with $Fe(NO_3)_3{\cdot}9H_2O$ (0.202, 0.5 mmol) in a mixture of methanol (20 mL) and ethanol (95%; 30 mL) and subsequent slow addition of (2 M; 1 mL KOH) to the stirred reaction mixture. Blue-purple crystals of **1** were grown by slow evaporation of the ethanol solution. Yield: 72% based on $Fe(NO_3)_3{\cdot}9H_2O$. Elemental analysis (%) calcd for $C_{41}Fe_2H_{63}K_3N_2O_{17}$, which corresponds to the crystallographically determined formula minus one water: C 45.39, H 5.85, N 2.58; found: C 45.66, H 6.41, N 2.83. FTIR: $\tilde{\nu}$ = 3679 (m), 3435 (s, br), 2955 (s), 2868 (w), 2814 (w), 1631 (vs), 1471 (m), 1440 (w), 1413 (w), 1375 (s), 1329 (m), 1308 (m), 1263 (m), 1243 (m), 1207 (m), 1171 (m), 1125 (m), 1085 (w), 1036 (s), 1008 (w), 980 (w), 961 (w), 916 (m) 892 (w), 875 (m) cm^{-1}.

2: Complex **2** was prepared by the reaction of hnida (0.08 g, 0.28 mmol) with $FeCl_3{\cdot}6H_2O$ (0.135 g, 0.5 mmol) in ethanol (95%, 30 mL) in the presence of potassium hydrogen carbonate (0.63 g, 6.3 mmol). Water (3 mL) was then added to assist the dissolution of the potassium hydrogen carbonate. Red-purple crystals of **2** were grown by slow evaporation of the solvent. Yield: 32% based on hnida. Elemental analysis (%) calcd for $C_{35}Fe_2H_{48}K_4N_2O_{22}$: C 37.64, H 4.33, N 2.51; found: C 37.31, H 4.22, N 2.57. FTIR: $\tilde{\nu}$ = 3557 (w), 3417 (s, br), 2967 (w), 2918 (w), 1598 (vs), 1507 (m), 1484 (m), 1460 (s), 1430 (m), 1398 (s), 1363 (s), 1309 (m), 1289 (sh), 1275 (s), 1243 (w), 1224 (w), 1174 (w), 1162 (w), 1144 (w), 1120 (w), 1099 (w), 1071 (m), 1046 (m), 1021 (m), 980 (w), 969 (w), 919 (m), 899 (w), 876 (w), 858 (m), 827 (m), 783 (w), 737 (s), 646 (m), 556 (m), 503 (m), 484 (m) cm^{-1}.

3: Complex **3** was prepared as reported previously.[8]

4: Complex **4** was prepared by the reaction of chnida (0.08 g, 0.24 mmol) with $FeCl_3{\cdot}6H_2O$ (0.135 g, 0.5 mmol) in a mixture of methanol (30 mL) and ethanol (95%; 20 mL) and subsequent slow addition of KOH (2 M; 2 mL) to the stirred reaction mixture. Red crystals of **4** were grown by slow evaporation of the solution. Yield: 36% based on chnida. FTIR: $\tilde{\nu}$ = 3412 (s), 3070 (sh), 2924 (w), 1621 (vs), 1597 (sh), 1558 (sh), 1500 (m), 1447 (m), 1428 (w), 1395 (s), 1365 (sh), 1291 (w), 1272 (m), 1210 (m), 1173 (w), 1154 (w), 1125 (w), 1097 (m), 1049 (w), 1024 (w), 978 (m), 930 (w), 906 (m), 862 (m), 815 (m), 743 (s) cm^{-1}.

5: Complex **5** was prepared by the dissolving of SO_3hda (0.08 g, 0.24 mmol) with $FeCl_3{\cdot}6H_2O$ (0.135 g, 0.5 mmol) in methanol (30 mL) and ethanol (95%; 20 mL) and subsequent slow addition of KOH (2 M; 2 mL) to the stirred reaction mixture. Red-brown crystals of **5** were grown by slow evaporation of the ethanol solution. Yield: 10–20% based on SO_3hda. FTIR: $\tilde{\nu}$ = 3475(br), 2576(m), 1610(s), 1480(s), 1385(s), 1295(s), 1213(s), 1183(s), 1132(s), 1104(s), 1034(s), 977(w), 934(w), 861(w), 794(w), 746(w) cm^{-1}.

Crystallographic data: Data measured on a STOE IPDS diffractometer for **1** and **2** or on a Bruker SMART Apex diffractometer for **4** and **5** at 200 K using graphite-monochromated $Mo_{K\alpha}$ radiation. The structure of **3** has been reported by us previously.[8] Structure solution by direct methods and full-matrix refinement against F^2 (all data) using SHELXTL.[18] Non-hydrogen atoms refined with anisotropic temperature factors apart from some disordered solvent molecules. The hydroxo hydrogen atom in **1** was located and refined, all organic ligand hydrogen atoms were placed in calculated positions. CCDC 262829–262832 contain the supplementary crystallographic data for this paper. These data can be obtained free of charge from the Cambridge Crystallographic Data Centre via www.ccdc.cam.ac.uk/data_request/cif.

1: $C_{41}H_{65}Fe_2K_3N_2O_{18}$, 1102.95 g mol^{-1}, purple-blue block 0.3 × 0.25 × 0.2 mm, T = 200 K, triclinic, $P\bar{1}$, a = 9.7594(8), b = 13.8993(11), c = 18.7162(16) Å, α = 97.662(10)°, β = 100.012(10)°, γ = 93.350(9)°, V = 2469.2(4) Å^3, Z = 2, $F(000)$ = 1156, ρ_{calcd} = 1.483 Mg m^{-3}, $\mu(Mo_{K\alpha})$ = 0.913 mm^{-1}, 16248 reflections measured ($2\theta_{max}$ = 52.0°), of which 9003 unique (R_{int} = 0.0897). 314 parameters, wR_2 = 0.1474, S = 0.921 (all data), R_1 (3984 data with $I > 2\sigma(I)$) = 0.0606.

2: $C_{35}H_{48}Fe_2K_4N_2O_{22}$, 1116.85 g mol^{-1}, purple block 0.25 × 0.2 × 0.15 mm, T = 200 K, triclinic, $P\bar{1}$, a = 8.6793(7), b = 15.1432(11), c = 17.9198(15) Å, α = 88.492(9), β = 76.093(9), γ = 74.962(9)°, V = 2206.3(3) Å^3, Z = 2, $F(000)$ = 1152, ρ_{calcd} = 1.681 Mg m^{-3}, $\mu(Mo_{K\alpha})$ = 1.121 mm^{-1}, 14611 reflections measured ($2\theta_{max}$ = 52.3°) of which 8112 unique (R_{int} = 0.0279). 625 parameters, wR_2 = 0.1202, S = 0.975 (all data), R_1 (5298 data with $I > 2\sigma(I)$) = 0.0690.

4: $C_{33}H_{49}Fe_2K_6N_2O_{31.5}$, 1324.04 g mol^{-1}, red cuboctahedron 0.2 × 0.2 × 0.2 mm, T = 200 K, rhombohedral, $R\bar{3}c$, a = 35.3692(10), c = 43.3010(18) Å, V = 46911(3) Å^3, Z = 36, $F(000)$ = 2444, ρ_{calcd} = 1.687 Mg m^{-3}, $\mu(Mo_{K\alpha})$ = 1.132 mm^{-1}, 63861 reflections measured ($2\theta_{max}$ = 52.0°) of which 10213 unique (R_{int} = 0.0798). 741 parameters, wR_2 = 0.4287, S = 1.348 (all data), R_1 (5085 with $I > 2\sigma(I)$) = 0.1294. Several crystals were investigated, and all gave a well-defined rhombohedral cell with systematic absences for $\bar{R}3c$. Structure solution readily gave the Fe_2 dinuclear complex and one or two of the K^+ counterions. However, refinement invariably resulted in high temperature factors for the atoms of the dinuclear unit, and indicated that all but one of the K^+ ions, and all the framework and lattice waters, were badly disordered, resulting in the high R-factors. Twinned refinement[19] in appropriate lower-symmetry rhombohedral or C-centered monoclinic space groups did not improve matters, and the problem is clearly one of disorder rather than (pseudo-)merohedral twinning. The final structure obtained, however, clearly establishes the formulation and the nature of the packing.

5: $C_{32}H_{76}Fe_2K_6N_2O_{40}S_2$, 1539.37 g mol^{-1}, red-brown prismatic needle 0.40 × 0.18 × 0.18 mm, T = 200 K, trigonal, space group $P3_221$, a = 20.8830(6), c = 12.4648(6) Å, V = 4707.6(3) Å^3, Z = 3, $F(000)$ = 2400, ρ_{calcd} = 1.629 Mg m^{-3}, $\mu(Mo_{K\alpha})$ = 1.026 mm^{-1}, 23724 reflections measured, of which 7108 unique (R_{int} = 0.0440). 332 parameters, wR_2 = 0.1551, S = 1.001 (all data), R_1 = 0.0561 (6232 data with $I > 2\sigma(I)$). One K^+ counterion was 50:50 disordered against a water molecule. One lattice MeOH molecule per asymmetric unit (two per dimer) could be located and refined, but the residual volume is consistent with an overall formulation with seven MeOH per dinuclear unit. Loss of these solvent molecules is facile on removal of crystals from the mother liquor.

Magnetism: The magnetic susceptibility of a polycrystalline powder of **5** was measured between 2 and 300 K with applied magnetic fields of 0.1 and 1 T using a Cryogenic S600 SQUID magnetometer. Data were corrected for the magnetism of the sample holder which was determined separately in the same temperature range and field, and the underlying diamagnetism of the sample was estimated from Pascal's constants. Magnetization measurements were performed on the same sample at 2.7 K with field up to 6.0 T.

Thermogravimetric analysis was performed under flowing N_2 and in a temperature range of 25–1000 °C using Rigaku ThermoPlus TG 8120 or Netzsch STA 409C instruments.

TEM studies were carried out on a JEOL FX2000. The sample was ground to a powder and placed on copper mesh for TEM analysis

(Accelerating voltage: 200 kV). Calibration was performed using a MoS_2 standard.

Received: February 10, 2005
Published online: June 14, 2005

Keywords: bridging ligands · coordination modes · crystal engineering · iron · supramolecular chemistry

[1] a) *Comprehensive Supramolecular Chemistry*, *Vols. 1–11* (Eds.: J.-M. Lehn, J. L. Atwood, J. E. D. Davis, D. D. MacNicol, F. Vögtle), Pergamon, Oxford, **1990–1996**; b) J.-M. Lehn, *Supramolecular Chemistry: Concepts and Perspectives*, VCH, Weinheim, **1995**.

[2] a) M. Eddaoudi, J. Kim, N. Rosi, D. Vodak, J. Wachter, M. O'Keeffe, O. M. Yaghi, *Science* **2002**, *295*, 469–472; b) N. L. Rosi, J. Eckert, M. Eddaoudi, D. T. Vodak, J. Kim, M. O'Keeffe, O. M. Yaghi, *Science* **2003**, *300*, 1127–1129; c) G. Férey, M. Latroche, C. Serre, F. Millange, T. Loiseau, A. Percheron-Guégan, *Chem. Commun.* **2003**, 2976–2977; d) D. N. Dybtsev, H. Chun, S. H. Yoon, D. Kim, K. Kim, *J. Am. Chem. Soc.* **2004**, *126*, 32–33; e) M. Fujita, Y.-J. Kwon, S. Washizu, K. Ogura, *J. Am. Chem. Soc.* **1994**, *116*, 1151–1152; f) J. S. Seo, D. Wand, H. Lee, S. I. Jun, J. Oh, Y. Jeon, K. Kim, *Nature* **2000**, *404*, 982–986.

[3] a) R. Robson, *J. Chem. Soc. Dalton Trans.* **2000**, 3735–3744; b) M. Fujita, K. Umemoto, M. Yoshizawa, N. Fujita, T. Kusukawa, K. Biradha, *Chem. Commun.* **2001**, 509–518; c) M. Fujita, *Chem. Soc. Rev.* **1998**, *27*, 417–425; d) M. Eddaoudi, D. B. Moler, H. L. Li, B. L. Chen, T. M. Reineke, M. O'Keeffe, O. M. Yaghi, *Acc. Chem. Res.* **2001**, *34*, 319–330; e) S. R. Seidel, P. J. Stang, *Acc. Chem. Res.* **2002**, *35*, 972–983; f) B. Olenyuk, A. Fechtenkötter, P. J. Stang, *J. Chem. Soc. Dalton Trans.* **1998**, 1707–1728; g) G. F. Swiegers, T. J. Malefetse, *Chem. Rev.* **2000**, *100*, 3483–3537; h) D. J. Price, A. K. Powell, P. T. Wood, *Dalton Trans.* **2003**, *12*, 2478–2482; i) S. O. H. Gutschke, D. J. Price, A. K. Powell, P. T. Wood, *Eur. J. Inorg. Chem.* **2001**, 2739–2741.

[4] a) O. M. Yaghi, M. O'Keeffe, N. W. Ockwig, H. K. Chae, M. Eddaoudi, J. Kim, *Nature* **2003**, *423*, 705–714; b) O. M. Yaghi, H. Li, *Angew. Chem.* **1995**, *107*, 232–234; *Angew. Chem. Int. Ed. Engl.* **1995**, *34*, 207–209; c) D. N. Dybtsev, H. Chun, K. Kim, *Angew. Chem.* **2004**, *116*, 5143–5146; *Angew. Chem. Int. Ed.* **2004**, *43*, 5033–5036.

[5] a) C. Livage, C. Egger, G. Férey, *Chem. Mater.* **2001**, *13*, 410; b) C. Livage, C. Egger, G. Férey, *Chem. Mater.* **1999**, *11*, 1546; c) D. J. Price, S. Tripp, A. K. Powell, P. T. Wood, *Chem. Eur. J.* **2001**, *7*, 200–208; d) S. O. H. Gutschke, D. J. Price, A. K. Powell, P. T. Wood, *Angew. Chem.* **2001**, *113*, 1974–1977; *Angew. Chem. Int. Ed.* **2001**, *40*, 1920–1923; e) N. Guillou, Q. M. Gao, P. M. Forster, J. S. Chang, S. E. Park, G. Férey, A. K. Cheetham, *Angew. Chem.* **2001**, *113*, 2913–2916; *Angew. Chem. Int. Ed.* **2001**, *40*, 2831–2834.

[6] a) P. M. Forster, P. M. Thomas, A. K. Cheetham, *Chem. Mater.* **2002**, *14*, 17–20; b) P. M. Forster, A. K. Cheetham, *Angew. Chem.* **2002**, *114*, 475–477; *Angew. Chem. Int. Ed.* **2002**, *41*, 457–459.

[7] See for example: a) B. Kersting, *Angew. Chem.* **2001**, *113*, 4110–4112; *Angew. Chem. Int. Ed.* **2001**, *40*, 3987–3990; b) W. Schmitt, C. E. Anson, R. Sessoli, M. van Veen, A. K. Powell, *J. Inorg. Biochem.* **2002**, *91*, 173–189; c) W. Schmitt, P. A. Jordan, R. K. Henderson, G. R. Moore, C. E. Anson and A. K. Powell, *Coord. Chem. Rev.* **2002**, *228*, 115–126; d) S. Laborda, R. Clérac, C. E. Anson, A. K. Powell, *Inorg. Chem.* **2004**, *43*, 5931–5943; e) F. Bramsen, A. D. Bond, C. J. McKenzie, R. G. Hazell, B. Moubaraki, K. S. Murray, *Chem. Eur. J.* **2005**, *11*, 825–831.

[8] W. Schmitt, C. E. Anson, J. P. Hill, A. K. Powell, *J. Am. Chem. Soc.* **2003**, *125*, 11142–11143.

[9] a) J. C. Ma, D. A. Dougherty, *Chem. Rev.* **1997**, *97*, 1303–1324; b) G. W. Gokel, L. J. Barbour, R. Ferdani, J. Hu, *Acc. Chem. Res.* **2002**, *35*, 878–886; c) G. W. Gokel, *Chem. Commun.* **2003**, 2847–2852.

[10] a) J. S. Seo, D. Wand, H. Lee, S. I. Jun, J. Oh, Y. Jeon, K. Kim, *Nature* **2000**, *404*, 982–986; b) M. Fujita, Y.-J. Kwon, S. Washizu, K. Ogura, *J. Am. Chem. Soc.* **1994**, *116*, 1151–1152.

[11] D. Bradshaw, T. J. Prior, E. J. Cussen, J. B. Claridge, M. J. Rosseinsky, *J. Am. Chem. Soc.* **2004**, *126*, 6106–6114.

[12] a) O. Kahn, *Molecular Magnetism*, Wiley-VCH, New York, **1993**; b) H. Weihe, H. U. Güdel, *J. Am. Chem. Soc.* **1997**, *119*, 6539–6543.

[13] All potassium β-ferrite $K_xFe_{22}O_{34}$ ($x = 2$–4) structures are hexagonal and are composed of spinel blocks separated by layers of potassium ions. Depending on the potassium ion content (x), variation in the packing of the spinel units gives a different lattice constant c (23.8 or 35.9 Å with $a = b = 5.9$ Å). In this case the best simulation of the XRD pattern are obtained with $c = 35.9$ Å confirming $x = 4$.[12a]

[14] a) Y. Joseph, G. Ketteler, C. Kuhrs, W. Ranke, W. Weiss, R. Schlögl, *Phys. Chem. Chem. Phys.* **2001**, *3*, 4141–4153; b) G. Ketteler, W. Ranke, R. Schlögl, *J. Catal.* **2002**, *212*, 104–111.

[15] P. G. Menon, B. Delmon in *Handbook of Heterogeneous Catalysis*, *Vol. 1* (Eds.: G. Ertl, H. Knözinger, J. Weitkamp), VCH, Weinheim, **1997**, p. 101.

[16] W. P. Addiego, W. Liu, T. Boger, *Catal. Today* **2001**, *69*, 25–31.

[17] V. Temkina, M. N. Rusina, G. F. Yaroschenko, M. Z. Branzburg, L. M. Timakova, N. M. Dyatlova, *Zh. Obshch. Khim.* **1975**, *45*, 1564–1570.

[18] G. M. Sheldrick, SHELXTL-NT, 5.1, Bruker Analytical X-ray Systems, Madison, WI, **1997**.

[19] a) R. Herbst-Irmer, G. M. Sheldrick, *Acta Crystallogr. Sect. B* **1998**, *54*, 443–449; b) R. Herbst-Irmer, G. M. Sheldrick, *Acta Crystallogr. Sect. B* **2002**, *58*, 477–481.

